# Mapping paleoflooded areas on evaporite playa deposits over sandy sediments (Tablas de Daimiel, Spain) using hyperspectral DAIS 7915 and ROSIS spectrometer data

A. Riaza*, R. Mediavilla*, E. Garcia-Meléndez**, M.Suarez**, A. Hausold***, U. Beisl***, H. Van der Werff****

*(*) Instituto Geológico y Minero de España (IGME), Rios Rosas 23, 28003 Madrid, Spain Ph: 3491 3475907; Fax: 3491 4426216*

*(**) Departamento de Geología, Universidad de Salamanca, Pza. de la Merced s/n, 37008 Salamanca, Spain*

*(***) DLR_ German Aerospace Research Establishment, Remote Sensing Data Centre, Oberpfaffenhofen, Postfach 1116, 82230 Weßling, Deutschland*

*(****) International Institute for Aerospace Survey and Earth Sciences (ITC), P.O.Box 6, 7500 AA Enschede, The Netherlands*

a.riaza@igme.es, r.mediavilla@igme.es, egm@usal.es, msuarez@usal.es, Andrea.Hausold@dlr.de, ulrich.beisl@landshut.org, wdwerff@itc.nl

*ABSTRACT- Open-system lakes developing marshes are sensitive environments to climate changes. Mineralogical climate markers such as gypsum and dolomitized carbonate are spatialy traced using hyperspectral imagery. Climate-dependent saline soils, carbonate , organic matter and iron oxide crusts have been mapped along different stages of flooding and emersion in the past 2000 years using DAIS and ROSIS spectrometer data. Spectral behaviour interacting and masking from various mineralogical components are described on laboratory spectra. Influence of landuse on the spatial spectral behaviour of paleoenvironments is discussed. A general outline of the past pools is drawn on the area surrounding the actual marsh, providing priceless data to use in further paleoclimate limnological research and in the development of new techniques for that research.*

## 1 INTRODUCTION

The Las Tablas de Daimiel Natural Park frames a lake at the head of the river Guadiana draining to the Atlantic, settled in the large plain of La Mancha in central Spain (fig.1). This continental dry plain is subject to a Mediterranean climate with dry summer and winter and relatively short rainy seasons in spring and autumn. Periods of drought are recurrent within the lapse of five years. It is a wetland with a linear morphology associated to an alluvial plain (Casado and Montes, 1995), resulting from two main interacting processes.First, the overflooding of the rivers Cigüela and Guadiana, which join at the Tablas de Daimiel. And second, the natural discharge of the underlying aquifer, through upwelling water at points locally termed "ojos" (eyes).

The recent sedimentological record of the Quaternary deposits in the area points to recent harsh paleoenvironmental conditions (2500-2300 years before present) with diminishing humidity and lowering of groundwater levels (García Antón et al, 1986). Intensive use of groundwater for cereal crop irrigation has produced a serious descent on the groundwater level and cover, an already irreversible environmental problem. Today the Tablas de Daimiel has long since ceased to be an upwelling groundwater area and has instead become a big pool of artificial water inflow (Llamas, 1998).

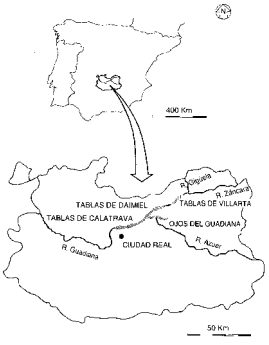


Fig 1. Geographical location of the Tablas de Daimiel wetland and natural park

Lakes are environments particularly sensitive to climate changes, both actual and paleoclimates. Open

system lakes fed by groundwater and seasonal runoff show a fluctuating shoreline.

The underlying most recent sediments are a system of sands deposited during the Holocene. The sand deposits present soil development of red-brown soils, considered remnants of old red soils now degraded (Pérez-González et al, 1983, Rodriguez García, 1998).

Organic sediments (peat) occur when the shallow channels excavated by the rivers overflow the adjacent floodplains with sediments loaded with clay, silt, sulphate, calcium and in lesser amounts, magnesium and chlorides. This favours the development of marshes on permanently flooded areas with abundant vegetation, where organic matter deposits occur. During the periods of draught, the groundwater level deepens, and the sediments are exposed developing saline soils with gypsum and dolomitization of carbonate. Water level fluctuations in open-system lakes cause much reworking of sediment in the nearshore zone (Allen and Collinson, 1978, in Reading, 1978).

Space and airborne imagery depicts subtle variations in the reflectance properties of desert surfaces, which are indicative of changes in mineralogical composition. The intensity of the red colour of sands in Namibia (Logan, 1960) has been used as an indication of age in the dunes. In Australia, the intensity of dune reddening resulted in information about the distance from the sand source area (El Baz, 1978; El Baz and Prestel, 1980).

The presence of hematite coatings on individual grains has been given as the cause of red colour in desert sands. Several studies indicate that the coating on sand grains is composed of kaolinite with powdery hematite, thus linking such reddening to desert varnish (Potter and Rossman, 1977). The hematite coating on quartz grains increases in thickness depending on the location of the deposit, and so the reddening of the sands increases with the transport distance (McCay et al, 1980. This way, the reddening property has been used to determine the relative ages of colour zones in the same sand field.

The effects of weathering processes on the spectral response of rocks exposed to the atmosphere has been evaluated both on sedimentary and igneous rocks on laboratory spectral measurements in the visible and nearinfrared (Riaza, 1992).

The mixtures of iron and clay minerals produced by weathering alteration associated to posthercynian erosion paleosurfaces in the Duero Basin (Central Spain) developed under different paleoclimates have been mapped using thematic mapper imagery (Riaza et al, 1997). Different image processing procedures helped to model sediment patterns on various stages of the evolution of the sedimentary basin (Riaza et al, 1995, 1997, 2000).

Iron bearing minerals, gypsum, carbonate and clays, have been used as the main mineral spectral references for the geological mapping of a carbonate area in the desert of Israel using the hyperspectral airborne spectrometer DAIS 7915 (Riaza et al, 1998).

Prior work has been focused on the spectral behaviour of playa evaporites both in the visible and nearinfrared (Crowley, 1991, 1993) and thermal infrared (Crowley, 1996). The influence of organic matter on soil colour is a long experienced relationship in spectrometry (Shields et al, 1968, Leone and Escadafal, 2001). Saline soils are recurrent on remote sensing studies because of their relationship with anthropic irrigation uses (Dehaan and Taylor, 2002; Koch et al, 2000). Various spectral libraries of minerals and rocks have been built, which are now in the public domain and well known by the geological community (Clark et al, 1993; Grove et al, 1992; Salisbury et al, 1992).

Areas flooded by water in the past which are nowadays exposed to the surface in the Tablas de Daimiel have changed the mineralogical and spectral aspect of the underlying Holocene sands, the most recent deposit hosting the wetland. The colour of the sand is darkened to grey, by influence of large amounts of organic matter deposited at the bottom of the flooded area. Meanwhile, peat and saline deposits are developed. Gypsum and carbonate precipitate (Arauzo et al, 1996), and new clays such as palygorskite and sepiolite occur. Such mineralogical changes can be spectrally detectable on the imagery.

## 2 METHOD

DAIS 7915 and ROSIS Spectrometer data were recorded on July 2000, aiming to minimum vegetation vigour and maximum soil exposure. The spatial resolution of 5 m for DAIS and 2 m for ROSIS was ensured at a flying altitude with maximum signal to noise ratio.

Non-coherent noise was corrected after in-flight calibration for DAIS (Strobl et al, 1996) to remove the sensor sensitivity effects on the 79 DAIS channels. Different spectral imaging processing tools were tested on atmospherically corrected data using a midlatitude summer profile (Richter, 1996; Richter et al, 2002) using field spectra from dark and light targets. ROSIS data with 115 channels in the visible 430-860 nm wavelength range, were corrected using a different procedure (Gege et al, 1998). Both sensors operated simultaneously at the same flight altitude. As a consequence, the area covered by ROSIS is a narrow belt centered along the DAIS central flightline (fig.12). The main interpretation procedures were focused on DAIS data. Particular nuances in the visible were contrasted with ROSIS data, with a 4 nm spectral resolution and 2 m spatial resolution compared to the 5 m DAIS spatial resolution.

Field spectra were collected for thematic analysis on geologically representative targets to be used for interpretative image processing with a GER Spectrometer. Non consolidated soil samples were collected at different stages during the interpretation of the imagery lead by hyperspectral image processing suggestions on mineralogy and sedimentology. Laboratory spectra were run on field soil samples using a Perkin-Elmer Lambda 6 Spectrometer in the visible and nearinfrared provided with an integrating sphere. Non consolidated rock samples were dry-sieved before measurement.

X-ray diffraction analysis was performed on selected non-consolidated rock samples to confirm field observations regarding mineralogical contents. Laboratory measurements were made on powdered samples after XRD aiming to ascertain spectral features which might appear on fine grained samples after separation of the clay fraction.

Image processing was conducted using ENVI hyperspectral modules and reference spectral libraries.

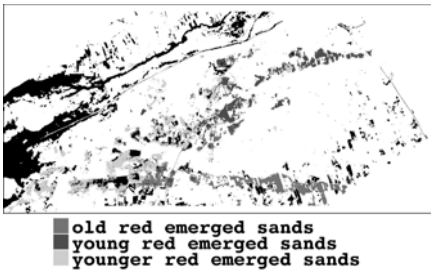


Fig.2. Geological map composed from DAIS images indicating the main sedimentary units

## 3 DIGITAL IMAGE PROCESSING

DAIS images were processed aiming to separate different sediments and minerals indicative of geological processes both of palustrine and fluvial environments (fig.2). Mosaics were composed with the two scenes for panoramic view of the area, and for selection of areas of interest (fig.3). Masks were built for densely vegetated areas using channels 17 and 13 for a red/nearinfrared ratio. Masks for water were also built using value 26 on channel 1 as threshold. A false colour composite with channels 19, 6 and 53 (BRG) was selected gathering both information on the three DAIS detectors on the visible and nearinfrared, and wavelength ranges which are critical for known reflectance absorptions diagnostic of minerals present in the area.

The six thermal infrared channels were used for a primary estimation of lithological variety (Riaza et al, 1998) (fig.3). Both Principal Components and Minimum Noise Fraction Transforms were useful identifying the main lithological regions indicating further hyperspectral image processing. Masks were built using selected minimum noise fraction transforms from thermal infrared channels to isolate geological units on the sands (fig.2). Pixel Purity Index and n-dimensional analysis were run on selected masked areas, helping to understand the geological spectral meaning of the various statistical populations among the sands (Boardman et al, 1993; Boardman and Kruse, 1994).

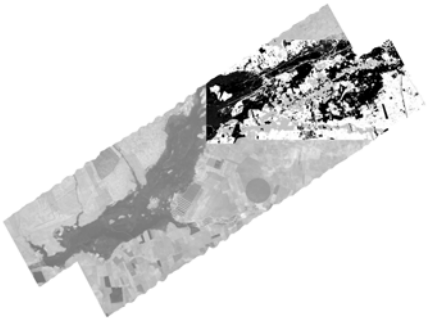

Fig.3. False colour composite with Principal components 1 (red), 2(green) and 3 (blue) computed from the six thermal infrared DAIS channels on the flight line mosaic after masking water and dense vegetation. Indication of the northeastern area selected for mapping.

Illumination Angle Effects jeopardised any subtle hyperspectral analysis on flightline mosaics. Image processing procedures were repeated for individual scenes and subsets, and maps were produced composing final results for the same geological units.

Field spectra taken with a GER Spectrometer were used with Spectral Angle Mapper (Kruse et al, 1993). Spectra showing iron absorption features were grouped into a library, and spectra showing carbonate absorptions were included into a different library. SAM was run on the 72 VIS-NIR DAIS channels on independent areas masked for the three main sandy areas: red emerged sands, depressions with organic matter, and flooded mudflats temporarily exposed developing saline soils (fig.4). The same procedure was used with the iron absorption library usingfirst only the 29 VIS DAIS channels, and the library with spectra showing carbonate absorptions was used to compute maps on the 2000-2500 nm wavelength range on a second stage (fig.5). Six representative spectra were selected after several attempts, giving better spatial outline of geological paleoflooded regions (fig.6).

The resulting maps were quite noisy when using a reduced number of channels, so that only maps computed with the 72 VIS-NIR channels were used for analysis. All results were very similar on the drawn geological units, coinciding with the spectral signatures

coming from PPI and n-dimensional analysis. SAM was more sensible showing the deeper flooded areas richer both in carbonates and organic matter (fig.4).


Fig.4. Map built using Spectral Angle Mapper on the grey mudflat "playa" sands on the 72 VIS-NIR DAIS channels using six selected field spectra taken with a GER spectrometer (fig.6). The deeper areas of the paleopool richer on organic matter and carbonate are isolated from the flooded mudflats on a fluctuating shore developing saline soils.

When using SAM on the red emerged areas (fig.5), a connecting channel among the two main paleopools is spectrally prominent. This connecting very shallow channel was not obvious on the prior analysis using mnf, ppi and n-dimensional analysis.

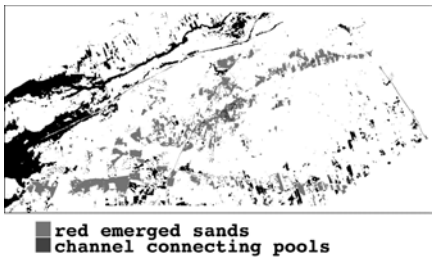


Fig 5. Map built using Spectral Angle Mapper on the red emerged sands on the 72 VIS-NIR DAIS channels using six selected field spectra taken with a GER spectrometer (fig.6). a channel connecting the two main paleopools is shown.

Laboratory spectra of nonconsolidated rock samples pointed to DAIS channels 33 (1520-1544 nm, gypsum), 34 (1565-1575 nm (gypsum), 40 (1777-1757, gypsum), 59 (2229-2225 nm, illite), 60 (2230-2240 nm, illite), 61 (2250-2253, gypsum, illite, palygorskite) and 64 (2298-2297 nm, sepiolite, dolomite) as critical showing absorptions related to minerals in the area (fig.8). Channels 41, 42 and 70 mineralogically sensitive to gypsum, goethite, calcite, illite and iron oxides, were rejected because of low signal quality. Hyperspectral image processing is impossible on this reduced number of channels, and more conventional image processing gives noisy results. However, useful hints came from colour composites built with mnf213 and pc214 from such channels.

The same procedure was used for ROSIS, elaborating parcial maps to contrast with DAIS results.

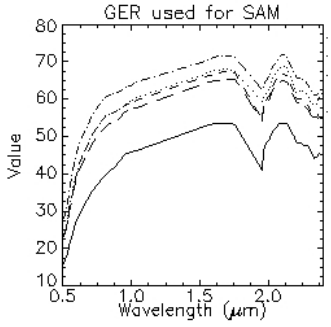


Fig 6. Field spectra taken with a GER spectrometer selected as depicting better geological units.

## 4 LABORATORY SPECTRA

Visual and mineralogical analysis of the fluvio-lacustrine system of the Tablas de Daimiel depicts a sulphate and carbonated water solution, being chloride absent. Intensive agricultural practices have destroyed any crusts which might have developed on the surface. Saline minerals are unstable mineralogical components, relying on subtle variations of temperature and humidity to precipitate or dissolve. Such physical parameters may change during daytime. Therefore, saline minerals excluding gypsum have not been used on the spectral interpretation, nor are crusts of any sort expected to be recorded by the imagery.

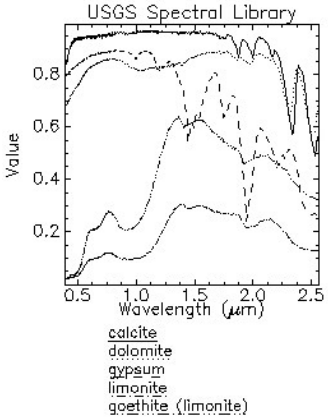


Fig.7. Spectra of the main minerals present on the sediments of the area of study related to palustrine and fluvial processes (United States Geological Survey Spectral Library).

The spectral response of mudflats around the former wetland are mineralogicaly dominated by gypsum and carbonate, whether calcite or dolomite (fig.7,8). Increasing dolomite contents would indicate an intensification of palustrine processes. Clays are not widely present in the area, nor does laboratory mineralogical analysis detect them.

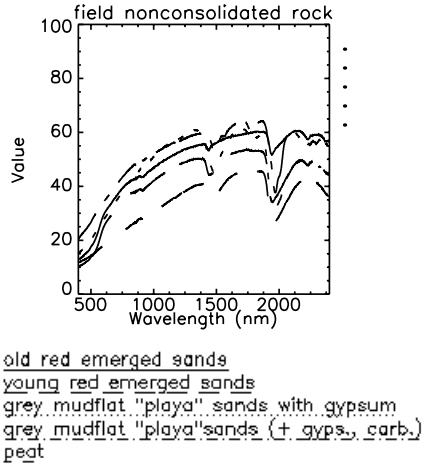


Fig.8. Laboratory Spectra from field nonconsolidated rock samples using a Perkin Elmer Lambda 6 Spectrometer on representative sediments, with expression of the minerals whose absorption features are present.

Laboratory spectra of peat is dominated by the presence of gypsum on typical shapes with minimum at 1477, 1520, 1565 and 2250 nm (Clark et al, 1992) (fig.7,8). The presence of carbonate appears as a weak 1975 nm minimum. Sepiolite and mainly dolomite are detected by the 2298 nm.

The holocene red sands are sediments composed of sand with quartz as a principal component. The overall reflectance of sands is higher than peat due to the influence of gypsum and saline minerals (fig.7,8). Clays are responsible for the 1438 nm minimum. Goethite contributes with a weak 1943 nm minimum and illlite to the 2229-2230 nm and weak 2370 nm minimum. X-ray diffraction analysis showed no presence of clays on the red sands, but rather and widespread carbonate. Spectra run on clay size powder from soil samples showed the presence of carbonate on most red sands (fig.9). Grey sands which had been once flooded also show the same carbonate absorption.

Several systems of red sands have been spectrally identified based on different iron minerals related to variable time of exposure to the atmosphere and weather conditions. Three morphosedimentary surfaces can be distinguished by intensity of reddening directly related to age (fig.8,10,11). Intense reddening occurs on older and topographically highest surfaces resulting on deeper iron absorptions in the visible and higher overall reflectance. Darker red colour on lower surfaces is associated to lower overall reflectance.

The grey sands, which have been once flooded by water present a dolomite 2298 nm minimum, absent on the rest of the sands (fig.8). XRD have revealed the presence of nesquehonite, a magnesium carbonate common as secondary mineral in saline playa deposits with high Mg/Ca ratios and high Mg concentration in water (Kelts and Hsü, 1978). The presence of dolomite is indicative of organic matter degradation, whether by oxidation liberating sulphur, or by increase of Mg in the system from runoff.

The spectral response of gypsum dominates grey sands, along with dolomite (fig.8). The displacement of a minimum from 1940 to 1970 nm indicates the transition from the temporarily flooded mudflat to the everemerged sands only subjected to reddening by iron coatings developed by exposure to the atmosphere. Spectra on powdered samples for X-ray diffraction analysis only display the gypsum absorption features when present. However, carbonate has been reported on the same samples. Gypsum dominates and hinders spectrally the presence of carbonate, both on soil samples and clay-size powdered samples (fig.8,9). The presence of gypsum on the grey sands increases geographically towards the river, indicating a likely progressive water salinity in comparatively recent times.

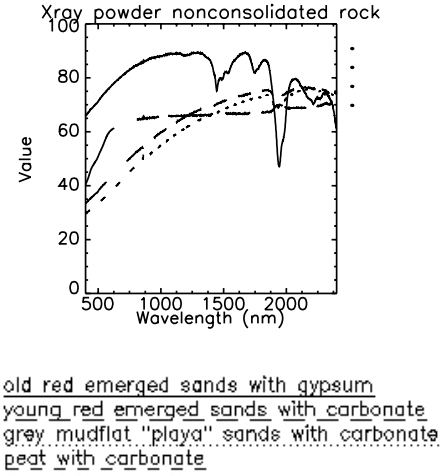


Fig.9. Laboratory Spectra from powder after X Ray Diffraction Analysis from field nonconsolidated rock samples, using a Perkin Elmer Lambda 6 Spectrometer on representative sediments, with expression of the minerals whose absorption features are present.

Peat, in spite of the high contents of organic matter, records spectrally the presence of gypsum

(fig.8). High contents of organic matter obliterates any spectral response from iron minerals (Galvao and Vitorello, 2001). Presence of carbonate is shown by spectra run on clay-size powdered samples for X-ray diffraction analysis (fig.9).

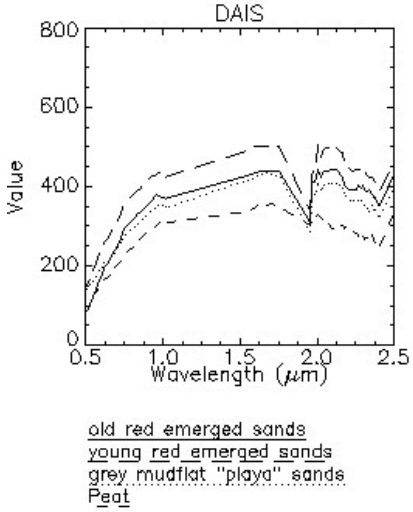


Fig.10. Z profiles from DAIS images from areas representing sedimentary units on maps built using digital image processing (fig.2 and 11).

Carbonate is widespread throughout the area, both in emerged and flooded areas. Imagery is quite noisy on the nearinfrared to be able to show carbonate-related absorption, relatively weak on the laboratory spectra. Hyperspectral profiles on DAIS imagery do not depict a clear spectral response due to the low energy available for the fourth detector on the 2000-2500 nm wavelength range. However, the topographically low areas where water was deeper and rich in gypsum should pop on the nearinfrared.

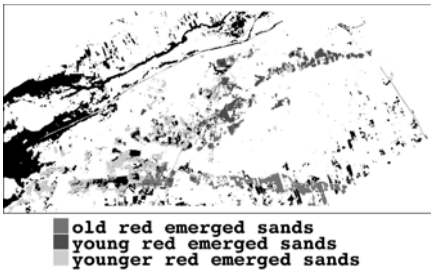


Fig.11. Geological map on red emerged sands built from DAIS imagery associated to three main morphosedimentary surfaces.

## 5 DAIS SPECTRAL RESPONSE

DAIS images present a distinguishing response from once flooded and everemerged areas (figs.10,11). All the emerged areas, whether sand deposits or continental aprons or fluvial deposits, show depressions in the visible due to the presence of iron bearing minerals.

The wide depression on red everemerged sands is more pronounced, consistent with their bright orange colour. In all of the mapped units, young red emerged sands display the highest overall reflectance. The areas which were once flooded are less expressive on the visible.

In the nearinfrared, the most distinguishing feature is the presence of a narrow absorption at 2.1 μm on areas which were flooded. Both bloedite $Na_2Mg(SO_4)_2.4H_2O$, calcite and dolomite can be responsible.

The areas which are emerged display a shoulder centred between 2.2-2.3 μm non-existent on the flooded areas. This might suggest abundance of clays, which is not confirmed by XRD mineralogical analysis or by sedimentological expectations. Widespread carbonate can also contribute to this spectral feature.

DAIS imagery show differences inside the flooded areas due to the variable contents on organic matter, gypsum and saline minerals (fig.4). The deeper hydrologically closed areas, where standing water persisted longer to develop marshes and to precipitate organic matter in detectible amounts, seem to be richer also in gypsum. When the groundwater level lowers, marshes are exposed to the atmosphere developing saline soils.

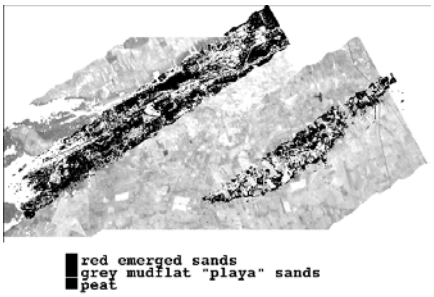


Fig. 12. Map built from ROSIS data using a similar procedure to former DAIS data, overlying over DAIS images, representing the main sedimentary units.

Preliminary analysis on DAIS imagery does not show distinctive absorptions among the mapped units, but Spectral angle Mapper using selected field spectra depicted subtle spectral variations (fig. 4). A depression on 2.3 μm is present on both peat and saline mudflats, whether due to gypsum or carbonate. The overall

reflectance is lower on the areas longer flooded due to more abundant organic matter.

## 6 ROSIS SPECTRAL RESPONSE

ROSIS data display a similar pattern of geological units when following the same digital image processing procedure used for DAIS (fig.12). Improved spatial resolution increases the spectral variability particularly on red emerged sands. Spectra do not display a very obvious iron absorption feature, due to the atmospherical correction system (fig.13).

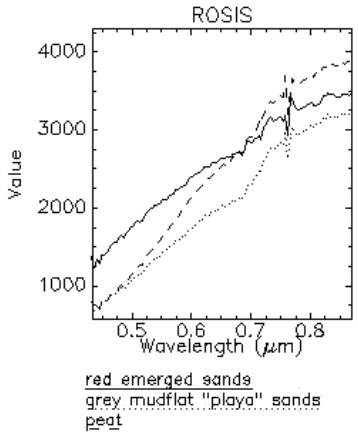


Fig. 13. Z profiles from ROSIS images from areas representing sedimentary units on maps built using digital image processing (fig. 12).

## 7 CONCLUSIONS

Hyperspectral imagery has been able to distinguish paleoflooded areas related to a receding wetland due to differential mineralogical contents associated with topography and palustrine and fluvial processes.

Gypsum, carbonate and organic matter are paleoclimate indicators spectrally recorded by the imagery in the VIS-NIR. Saline soils with gypsum both on occasionally overflooded areas adjacent to shallow river channels and on mudflats around standing water pools, have been recorded by the imagery. Originally deeper areas rich in organic matter where marshes develop at times of low water movement are also shown.

Gypsum masks the presence of carbonate on the spectral response. Only X-ray diffraction analysis has depicted the presence of carbonate when coexisting with gypsum. Therefore, carbonate may also be present in the geochemically central fluvio-lacustrine areas rich in gypsum.

Several systems of fluvial terraces with red sands have been shown by the imagery. Mineralogical variations on iron oxides and hydroxides developed when sediments are emerged in periods of drought are easily recorded in the visible wavelength range.

DAIS thermal infrared, particularly sensitive to topography, was first used to depict spectrally variable areas. From them, through successive hyperspectral image processing on selectively masked areas, a spatial map of the paleolake has been drawn from the imagery, orientating drill location for further palinological studies and paleoenvironmental analysis.

## 8 ACKNOWLEDGEMENT

The Fifth Framework Program, Improvement of Human Potential, Access to Research Infrastructures (contr. HPRI-CT-1999-00075, ref HS2000-ES1) funded data for this work. Thanks are due to S. Martin Alfageme and Iñigo Martin for software and hardware assistance (STIG, University of Salamanca). J. O´Malley reviewed the English version.

## 9 REFERENCES

Allen , P.A. and Collinson, J.D., 1978, Lakes.In., Sedimentary Environment and Facies, edited by H.G. Reading (Oxford, London: Blackwell Scientific Publications), pp 63-282.

Boardman, J. W., 1993, Automated spectral unmixing of AVIRIS data using convex geometry concepts. In Summaries Fourth JPL Airborne Geoscience Workshop, JPL Publication 93-26, v. 1, pp. 11 - 14.

Boardman J.W. and Kruse, F. A., 1994, Automated spectral analysis: A geologic example using AVIRIS data, north Grapevine Mountains, Nevada: in Proceedings, Tenth Thematic Conference on Geologic Remote Sensing, Environmental Research Institute of Michigan, Ann Arbor, MI, pp. I-407 - I-418.

Arauzo, M., Rubio, A., and Vicioso, J., 1996, El ambiente acuático: Hidroquímica, 70-90, in Alvarez Cobelas, M. y Cirujano, S., Ed., Las Tablas de Daimiel, Ecología Acuática y Sociedad, Ed. Organismo Autónomo Parques Nacionales, Madrid, 370 p.

Casado, S. and Montes, C., 1995, Guía de los lagos y humedales de España, Reyero, Madrid, 255 p.

Garcia Antón, M., Morla, C., Ruiz Zapata, B., Sais Ollero, H., 1986, Contribución al conocimiento del paisaje vegetal Holoceno en la Submeseta Sur Ibérica: análisis polínico de sedimentos

higroturbosos en el Campo de Calatrava (Ciudad Real, España), In:Quaternary Climate in Western Mediterranean (F. López Vera ed.), Universidad Autónoma de Madrid Publications.

Clark, R. N., Swayze, G. A., Gallagher, A., King, T. V. V. and Calvin, W. M., 1993. The U.S. Geological Survey Digital Spectral Library: Version 1: 0.2 to 3.0 mm: U.S. Geological Survey, Open File Report 93-592, 1340 p.

Crowley, J.K. and Hook, S.J., 1996, Mapping playa evaporite minerals and associated sediments in Death Valley, California, with multispectral thermal infrared images, Journal of Geophysical Research, vol.101, no. B1, 643-660, January 10.

Crowley, J.K., 1993, Mapping playa evaporite minerals with AVIRIS data: A first report from Death Valley, California, Remote Sensing of Environment, 44, 337-356.

Crowley, J.K., 1991, Visible and near-infrared (0.4-2.5 μm) reflectance spectra of playa evaporite minerals, Journal of Geophysical Research, 96, 16.231-16.240.

Dehaan, R.L. and Taylor, G.R., 2002, Field-derived spectra of salinized soils and vegetation as indicators of irrigation-induced soil salinization, Remote Sensing of Environment 80, 406-417.

El Baz, f., 1978, The meaning of desert color in earth orbital photographs, Photogrametric Engineering and Remote Sensing, 44, 69-75.

El Baz, F., Prestel, D.J., 1980, Desert varnish on sand grains from the Western Desert of Egypt: Importance of the clay component and implications to Mars. In : Lunar and Planetary Science XI, 1980, Houston, Texas: Lunar and Planetary Institute, 254-256.

Galvao, L.S., and Vitorello, I., 1998, Role of organic matter in obliterating the effects of iron on spectral reflectance and colour of Brazilian tropical soils, International Journal of Remote Sensing, 19, nº 10, 1969-1979.

Garcia Antón, M., Morla, C., Ruiz Zapata, B., Sais Ollero, H., 1986, Contribución al conocimiento del paisaje vegetal Holoceno en la Submeseta Sur Ibérica: análisis polínico de sedimentos higroturbosos en el Campo de Calatrava (Ciudad Real, España), In:Quaternary Climate in Western Mediterranean (F. López Vera ed.), Universidad Autónoma de Madrid Publications.

Gege, P., Beran, D., Mooshuber, W., Schulz, J., van der Piepen, H., 1998, System analysis and performance of the new version of the imaging spectrometer ROSIS, Proceedings 1st Workshop on "Imaging Spectroscopy", Zürich, Switzerland, 6-8th October 1998, 29-36.

Grove, C. I., Hook, S. J., and Paylor II, E. D., 1992. Laboratory Reflectance Spectra of 160 Minerals, 0.4 to 2.5 Micrometers: Jet Propulsion Laboratory Pub., 92-2.

Kelts, K., and Hsü, K.J., 1978, Freshwater Carbonate Sedimentation, In Lerman, A., ed. "Lakes: chemistry, geology, physics", Springer Verlag, 1978, New York, 363 p.

Koch, M., 2000, Geological controls of land degradation as detected by remote sensing: a case study in Los Monegros, north-east Spain, International Journal of Remote Sensing, 21-3, 457-474.

Kruse, F. A., Lefkoff, A. B., Boardman, J. B., Heidebrecht, K. B., Shapiro. A. T., Barloon, P. J., and Goetz, A. F. H., 1993. The Spectral Imaging Processing System (SIPS) – Interactive Visualization and Analysis of Imaging Spectrometer Data, Remote Sensing of Environment, 44, 145-163.

Leone, A.P., and Escadafal, R., 2001, Statistical analysis of soil colour and spectroradiometric data for hyperspectral remote sensing of soil properties (example in a southern Italy Mediterranean ecosystem), International Journal of Remote Sensing, 22, nº12, 2311-2328.

Logan, R.F., 1960, The Central Namib Desert, National Academy of Sciences, National Research Council Publication 785, 162 p.

Llamas, M.R., Conflicts Between Wetland Conservation and Groundwater Exploitation: Two Case Histories in Spain, 1988, Environmental Geology and Water Science, vol.11, nº 3, 241-251.

Mathieu, R., Pouget, M., Cervelle, B. and Escadafal, R., 1998, Relationships between Satellite-Based Radiometric Indices Simulated Using Laboratory Reflectance Data and Typic Soil Color of an arid Environment, Remote Sensing of Environment, 66, 17-28.

McCay, D., Constantonopolus, C., Prestel, DJ. and El Baz, F., Thickness of coatings on quartz grains from the Great Sand Sea, Egypt. In Reports of

Planetary Geology Program- 1980, Washington D.C.: National Aeronautics and Research Administration, NASA TM-82385, 1980, 304-306.

Pérez González, A., Aleixandre, A., Pinilla, J., y Gallardo, J., 1983, El pasaje eólico de la llanura aluvial de San Juan (llanura manchega central), Actas de la VI Reunión del Grupo Español de Trabajo en el Cuaternario, Galicia, 631-655.

Portero García, J.M., Ancochea, E., y Gallardo, J., 1988, Memoria del Mapa Geológico a escala 1:50.000, Segunda Serie, hoja nº 760 (Daimiel).

Potter, T.R. and Rossman, J.R., 1977, Desert varnish: the importance of clay minerals. Science, 196, 1446-1448.

Riaza, A., 1992, Reflectancia en rocas en función de su litología y fábrica interna. II Cartografía de rocas ígneas en el Complejo de Burguillos del Cerro en el visible y el infrarrojo cercano: reflectancia espectral en el laboratorio y evaluación estadística de la misma en relación con imágenes thematic mapper, Boletín Geológico y Minero, 103, n.3, 3-26.

Riaza, A., Mediavilla, R., Santisteban, J. L., Villar, P. and Martín Alfageme, S., 1995. Regolitos en una cuenca terciaria. Propiedades espectrales según su mineralogía en función de la evolución climática, Coloquio Internacional sobre propiedades espectrales y teledetección de los suelos y rocas del visible al infrarrojo medio, La Serena (Chile), 24-27 de Abril 1995, 100-104.

Riaza, A., Mediavilla, R., and Santisteban, J.I., 2000, Mapping geological stages of climate-dependent iron and clay weathering alteration and lithologically uniform sedimentary units using Thematic Mapper imagery, International Journal of Remote Sensing, vol.21, nº5, 937-950

Riaza, A., Mediavilla, R., Santisteban, J. L., Villar, P. and Martín Alfageme, S., 1997. Cartografía de formaciones geológicas litológicamente similares en zonas llanas cultivadas, V Reunión Científica de la Asociación Española de Teledetección, Las Palmas (Gran Canaria), 10-12 November 1993, 863-876.

Riaza, A., Kaufmann, H., Zock, A. and Müller, A., 1998, Mineral Mapping in Maktesh_Ramon (Israel) using DAIS 7915, Proceedings 1st EARSeL Workshop on Imaging Spectroscopy, Zürich, Switzerland, 6-8 October 1998, in press.

Richter, R., 1996. Atmospheric correction of DAIS hyperspectral image data, Computers & Geosciences, vol.22, no.7, 785-793.

Richter, R., Müller, A. and Heiden, U., 2002, Aspects of operational atmospheric correction of hyperspectral imagery, International Journal of Remote Sensing, vol.23, nº 1-10, 145-158.

Rodriguez García, J.A., 1998, Geomorfología de las Tablas de Daimiel y del endorreismo manchego centro-occidental, October 1998, MSc Thesis, University Complutense of Madrid, 164 p, unpublished.

Salisbury, J. W., Walter, L. S., Vergo, N. and D'Aria, D. M. 1992. Infrared (2.1-25 μm) Spectra of Minerals, The John Hopkins University Press, Baltimore (Maryland, USA).

Strain, P.L., El Baz, F.: 1982, Sand distribution in the Kharga depression of Egypt: Observations from Landsat images. International Symposium on Remote Sensing of Environment, 1982. Ann Arbor, Michigan: Environmental Research Institute of Michigan, First Thematic conference: Remote Sensing of Arid and Semi-arid Lands, Cairo, Egypt, ERIM, paper B-11, 101-102.

Strobl, P., Richter, R., Lehman, F., Müller, A., Zhukov, B., Oertel, D., 1996. Preprocessing for the Digital Airborne Imaging Spectrometer DAIS 7915, SPIE´s AEROSENSE ´96 Conference, Orlando, Apr. 8-12, 1996, SPIE Proc. Vol. 2758.

Shields, J.A., Paul, E. A., Arnaud, R.J.Sr. and Head, W.K., 1968, Spectrophotometric measurement of soil color and its relationship to moisture and organic matter, Canadian Journal of Soil Science, 48, 271-280.

Walker, T.R., 1967, Formation of red beds in modern and ancient deserts. Geological Society of America Bulletin, 78, 353-368.